JOURNAL OF AIRCRAFT
Vol. 32, No. 4, July–August 1995

Neural Network Approach to Fatigue-Crack-Growth Predictions Under Aircraft Spectrum Loadings

R. M. V. Pidaparti* and M. J. Palakal†
Purdue University at Indianapolis, Indianapolis, Indiana 46202

An artificial neural network (NN) method is developed to represent the fatigue-crack-growth and cycle relationships under spectrum loadings of the Mirage aircraft operated by the Royal Australian Air Force. This method utilizes load cycle spectrum using available flight and experimental data for crack growth vs cycles as input. The trained network is able to predict the relationship between the crack-growth and the loading cycles. The neural network is able to predict the crack-growth cycle behavior for different variations in the original loading spectrums. The results predicted by the NN model seem reasonable and the model is capable of representing crack-growth behavior for various arbitrary aircraft spectrum loadings with certain limitations. In addition, an attempt is made to predict the material parameters for Walker's fatigue-crack-growth relationship using a different neural network. Because of the demonstrated performance, it is possible that the proposed NN approach can be extended with more research effort to estimate the fatigue life of arbitrary cracked structural components under complex loadings in real time.

Nomenclature

a	=	crack length, in.
B	=	specimen thickness, in.
C	=	Walker crack-growth rate constant, constant
da/dN	=	fatigue-crack-growth rate, in./cycle
K	=	stress intensity factor, ksi$\sqrt{\text{in.}}$
m	=	Walker stress ratio exponent, constant
N	=	loading cycles, cycles
n	=	Walker equation's exponent, constant
P	=	uniaxial load on specimen, lb
r	=	stress ratio, constant
W	=	specimen width, in.
ΔK	=	stress intensity factor range, ksi$\sqrt{\text{in.}}$
σ	=	applied stress, psi

I. Introduction

MOST aircraft are subjected to different spectrum loadings throughout their flight regime. These loadings have a significant effect on their performance and life. Due to the large cracks that develop in certain aircraft because of fatigue loadings, flight loading limits were imposed to reduce the risk of in-flight structural failures and to reduce the crack-growth rate. These limits were in the form of a g limit, also referred to as a "placard" limit. Their effect was to truncate the maximum positive load levels in the loading spectrum. Removing certain peak loads has the potential for decreasing the life due to the loss of beneficial fatigue-crack retardation effects. Experimental and analytical studies showed that variations in flight loading had the potential for reducing beneficial retardation effects.[1] The delay or retardation effect on crack growth from a single peak tensile over a single load and multiple overloads are given in Refs. 2 and 3. The greater the magnitude of the overload, the greater the delay effect on fatigue-crack growth up to a sufficiently large overload.[2] The delay effect due to spectrum load sequence was studied by and showed the relation of fatigue-crack-growth retardation behavior due to crack-closure phenomena.

Received Aug. 18, 1993; revision received May 31, 1994; accepted for publication Feb. 3, 1995.

*Associate Professor, Department of Mechanical Engineering. Senior Member AIAA.

†Associate Professor, Department of Computer Science.

The fatigue-crack-growth mechanism involves a crack growth by a minute amount in every load cycle. Crack-growth life is expressed as the number of cycles required to grow a fatigue-crack over a certain distance. To determine the fatigue-crack-growth behavior, fatigue experiments are usually conducted on cracked specimen/components and the crack length a is plotted against the corresponding number of cycles N at which the crack is measured. The crack-growth rate da/dN (average length/cycles) is obtained by taking the derivative of the above crack length a vs cycles N curve. The crack-growth rate is a function of stress intensity factor range ΔK and stress ratio r (defined as $\sigma_{\min}/\sigma_{\max}$). This relationship is given as

$$\frac{da}{dN} = f(\Delta K, r) \tag{1}$$

where ΔK is a function of applied stress range $\Delta\sigma$ ($\sigma_{\min} - \sigma_{\max}$), geometry of the crack $f(g)$, crack size a, etc. The minimum stress $\sigma_{\min}$ and maximum stress $\sigma_{\max}$ are obtained from constant amplitude or variable amplitude spectrum loading. The ΔK relation is given by

$$\Delta K = K_{\max} - K_{\min} = f(g)\Delta\sigma\sqrt{\Pi a} \tag{2}$$

A plot of log da/dN vs log ΔK is a sigmoid curve. The majority of the fatigue life is taken up in propagation of a crack. Many structures/components operate in this region of crack propagation. By the use of fracture mechanics principles it is possible to predict the number of cycles in growing to a critical crack size or to find final failure.

The problem of fatigue-crack-growth behavior representation is complex and exhibits a nonlinear relationship between the crack-growth and loading cycles as given above. Most of the crack-growth models are based on empirical data. As an alternative to mathematical description, it will be of interest to use the neural network (NN) approach to represent the complex fatigue-crack-growth behavior for aircraft spectrum loadings.

An attempt has been made in this study to predict the relationship between the crack-growth and loading cycles using a novel computational paradigm based on artificial neural network models. NN is a paradigm for computation and knowledge representation inspired by the neuronal architecture and operation of the human brain. There have been

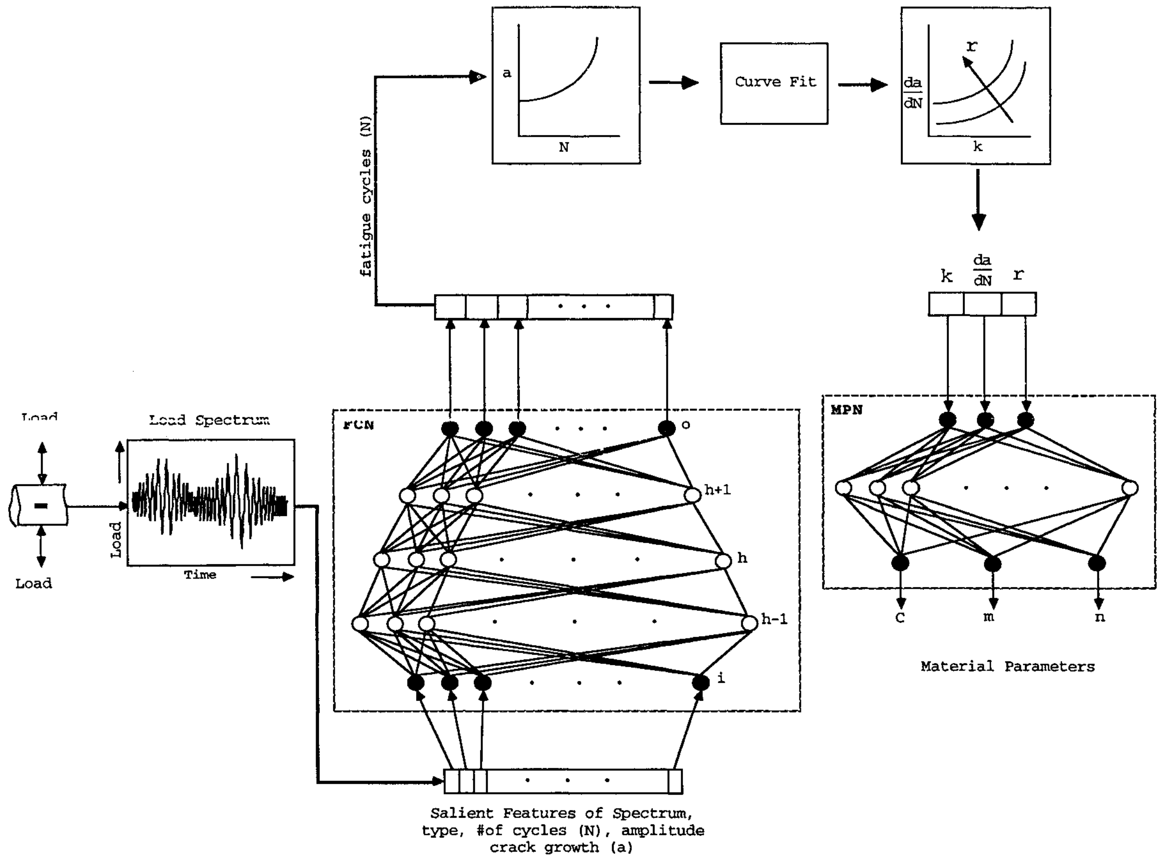

Fig. 1 Fatigue-crack-growth representation model using NN.

considerable research efforts in different applications of NN in the past: signal processing,[5] robotics,[6] structural analysis and design,[7] and pattern recognition,[8,9] to name a few. Other related work in the use of NN for effective modeling of a complex, highly nonlinear relationship among data sets can be found in Ref. 10. The resurgence of earlier research in NN has also facilitated the development of a novel approach to the derivation and representation of material behavior.[11,12] With this new approach, the knowledge of the materials behavior is captured within the connections of a learning NN that has been trained with experimental data. Recently, the NN approach was used to estimate the fatigue life of simple mechanical components.[13]

The objective of this study is twofold: 1) to represent the fatigue-crack-growth behavior under spectrum loadings using a NN model, and 2) to predict the material parameters for Walker's fatigue-crack-growth equation.[14] The essential features of a spectrum loading as well as the corresponding crack-growth behavior based on experimental data[15] are used as input to the network. The trained network is tested using different variations in spectrum loadings. The accuracy of the results obtained demonstrates that the NN method is a feasible approach for estimating the fatigue-crack-growth behavior and material parameters.

II. Fatigue-Crack-Growth Representation Model

Figure 1 shows a NN-based fatigue-crack-growth representation model for arbitrary spectrum loadings. This model is intended to predict the crack-growth behavior as well as the material parameters that fit into a relationship for cracked structural components. The NN model is based on the experimental data of crack growth vs loading cycles for a particular material. This NN approach is very useful for real-time estimates of critical crack lengths for the remaining loading cycles for operation of the cracked component or structure after it is generalized with experimental data. The model consists of two neural networks: 1) fatigue-crack-growth network (FCN) and 2) material parameters network (MPN), as shown in Fig. 1.

A. FCN

The underlying approach toward developing a NN-based fatigue-crack-growth behavior is to train a NN to map the relationship between crack growth and the number of loading cycles. The results from the experimental data for a particular material serve as input data to the network. The trained network would contain sufficient information about the material's crack-growth behavior. This trained network could be qualified as a model when the network is able to reproduce the trained data as well as other data for generalization.

The FCN receives the information about the features in the spectrum loading and crack-growth behavior for a particular cracked component and outputs the corresponding loading cycles. It is also possible to include a preprocessor before the FCN to extract salient features of the loading spectrum. However, in this present study, the salient features like peak amplitudes and location were used as the features for input to the FCN. The results from the FCN are processed by a postprocessor, in this case, a curve fit to generate the crack-growth rate da/dN curve.

B. MPN

The objective of this neural network is to find the material parameters that fit into the Walker equation.[14] Experimental data of ΔK and da/dN for different values of stress ratio and spectrum loadings are used to fit the Walker equation. The Walker equation is well known and takes into account the effect of stress ratio on crack-growth behavior for an applied ΔK, and is given by

$$\frac{da}{dN} = C[(1 - r)^{m-1}\Delta K]^n, \qquad r \geq 0.0 \tag{3}$$

where C, m, and n are material constants.

The results of da/dN vs ΔK curve for a particular stress ratio r are used as inputs to the MPN. The MPN processes these data to give the required material parameters. In the present study, Walker's fatigue-crack-growth equation, which is defined in terms of three material parameters C, m, and n, was used. However, the present approach can be extended to include other fatigue-crack-growth relationships. Both FCN and MPN have a different network architecture; i.e., different sets of I/O nodes and middle layers. The model presented here serves as an alternate to the existing mathematical or empirical models for fatigue-crack-growth representation based on the experimental data.

The distinctive features of the NN approach for fatigue-crack-growth representation are generalization, speed, and robustness or fault tolerance. Generalization ability lies in utilizing the network, after it has been trained, for variations on other arbitrary spectrum loadings that are not closely related to the training set. The parallel architecture of NN enables it to compute rapidly the critical crack lengths or loading cycles (fatigue life) in real time. Because of its distributed nature, the NN implementation of the fatigue-crack-growth relationship is expected to be robust and reliable. The details and implementation procedures for the FCN and MPN are discussed in the following sections.

III. Artificial Neural Networks

Artificial NNs are computational models that are modeled after the functionality of the human brain. It consists of a large number of highly interconnected artificial neurons called the processing units. Each processing unit, acting as an idealized neuron, receives input from the units to which it is connected, computes an activation level, and transmits nonuniformly transformed activation to other processing units. The I/O of a NN computation is represented by the activation level of designated I/O units, respectively. What the network computes is highly dependent on how the units are interconnected and the strength of the connections between them.

The NN derives the knowledge through presentation of examples, training cases, and the application of their self-organization capabilities. Different types of networks are possible by varying the number of nodes and their connectivity and the form of learning rules and activation functions that are used in the NN architecture. Artificial NN models are loosely classified into four different categories based on their learning qualities (unsupervised or supervised learning) and recall qualities (feedback or feed-forward recall).[10] Various NN models developed under these categories have been successfully applied in solving problems in several application areas such as signal analysis and processing, process control, robotics, pattern classification, noise filtering, speech processing, medical diagnosis, and many others.[10]

Among all other NN models developed thus far, back-propagation (BP) NN models have been very successful in solving various engineering and pattern recognition problems. The BP network is a feed-forward, multilayered network consisting of an input layer, one or more hidden layers, and an output layer. Each layer consists of several artificial neural cells. Each neuron cell consists of three main components: 1) a set of inputs, 2) a summation function, and 3) a transfer function to deliver an output. A back-propagation NN is used in this study to represent the fatigue-crack-growth relationships as well as for material parameter predictions under arbitrary spectrum loadings.

In order to describe the learning process in detail, consider the organization of a single artificial neuron unit (unit j at layer h of FCN of Fig. 1) shown in Fig. 2. Every unit in the FCN model is identical to the one shown in Fig. 2. Each unit also has identical connectivity and a certain computational property. For example, each unit in a given layer h is connected by all units in layer $(h - 1)$. Each connection has a weight W_{ij}^h, weight on connection joining ith unit in layer

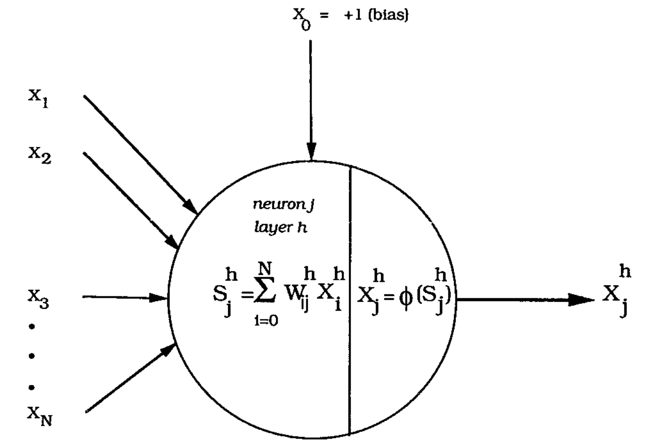

Fig. 2 Organization of an artificial neuron unit in a fatigue-crack-growth network.

$(h - 1)$ to the jth unit in layer h, associated with it. Each unit j has an output state X_j, which is a weighted sum of inputs to this particular unit. Using the representative unit shown in Fig. 2, the learning algorithm for FCN can be summarized as follows:

1) Present the input vector $x_1, x_2, \ldots, x_N$ to the input layer. This layer of the FCN has 84 input units. Each input unit receives a unique input item that corresponds to the salient features of the spectrum: variation of amplitudes with time, crack size, etc.

2) The next step is to calculate the output of unit j in layer h. In order to do this, first compute the summation value S for unit j in layer h using the equation

$$S_j^h = \sum_{i=1}^{N} W_{ji}^h X_i^{h-1} \tag{4}$$

and then calculate the output of this unit as

$$X_j^h = \phi(S_j^h) \tag{5}$$

where ϕ is a transfer function. In this implementation ϕ is used as a sigmoid function, which is given by

$$\phi(z) = (1.0 + e^{-z})^{-1} \tag{6}$$

The previous step is performed on all units at all three layers and up to the output layer.

3) At the output layer, calculate the actual output value o, in this case the number of N, for each unit k and then calculate a global error E using the equation

$$E = 0.5 \times \sum_{k=1}^{M} (t_k - o_k)^2 \tag{7}$$

where t is the desired output and o is the actual output for a given input vector i. E defined in Eq. (7) corresponds to a global error of the network for a particular (i, t). The aim of the learning process is to minimize E of the network by modifying the connection weights.

4) The modification of connection weights is accomplished based on knowledge of the local error at each processing unit and back-propagating this error information to the previous layers. The connection weight change is computed using the equation

$$\Delta W_{ij}^h = \eta \times \delta_j^h \times x_i^{h-1} \tag{8}$$

where δ_j is the term used to back-propagate errors in the hidden layer and η is the learning coefficient. The δ_j term is given by

$$\delta_j^h = x_j^h(1 - x_j^h) \sum_k \delta_j^{h+1} W_{kj}^{h+1} \tag{9}$$

The main idea here is to forward-propagate the input through the layers to the output layer, determine the error at the output layer, and then back-propagate the errors back through the network from the output layer to the input layer using the previous equation.

5) The final step now is to update all weights in the network by adding the current delta weights to the previous weights using the equation

$$\Delta W_{ij}^h = \eta \times \delta_j^h \times x_i^{h-1} + \alpha \Delta W_{ij}^{h-1} \tag{10}$$

where α is a momentum term that is used to speed-up the convergence while avoiding instability.

The process of forward-feeding the input and back-propagating the error will continue until the error at the output nodes is zero or is within an acceptable range. At this point the network is said to be converged.

IV. Implementation

Center-cracked specimens of 7075-T651 aluminum alloy subjected to loading spectrums of the Mirage aircraft operated by the Royal Australian Air Force were used to determine the effect on fatigue-crack-growth behavior by imposing a flight loading or placarded g limit. The maximum and minimum stress intensity factor for the center-cracked specimen is calculated as

$$K = \sigma\sqrt{\pi a}\ \sec(\pi a/W) \tag{11}$$

The experimental data reported in Ref. 15 was used to train the FCN. The FCN shown in Fig. 1 is modeled as a back-propagation NN that has three hidden layers. The NN architecture used in this study was based on empirical results as there are no rules available in the literature. The FCN developed in this investigation has one input layer with 84 nodes, three middle layers with 125, 65, and 45 nodes, respectively, and one output layer with 12 nodes (84-[125-65-45]-12).

The 84 input parameters chosen in this study are based upon various spectrum loading characteristics. For example, the first value represents the number of cycles and the second and third values correspond to the maximum and minimum amplitude of that particular cycle. Each spectrum has a four-flight loading sequence: CBAA′. This way, e.g., loading C contributes to 9 inputs (3 types of cycles and their corresponding maximum and minimum amplitudes), loadings B, A, and A′ have 15, 21, and 27 inputs, respectively, and 12 crack-growth increments (total input to the NN being: 9 + 15 + 21 + 27 + 12 = 84). The 12 output nodes represent the number of loading cycles corresponding to the 12 crack-growth increments in input nodes. Details of input data organization for the FCN are described in the next section.

Learning or training involves presenting the network with the experimental data such that it correctly reproduces the number of cycles for predetermined crack-growth lengths for each of the spectrum loadings. It was discovered that an effective way to train the NN is to present the data in normalized form. In this study, the number of cycles and the crack lengths in the data set were normalized between 0 and 1. This normalization allowed the trained NN to generalize better, and hence, generated more accurate results during the testing process.

Figure 3 shows the various Mirage spectrum loadings considered in this study.[15] These include constant amplitude spec-

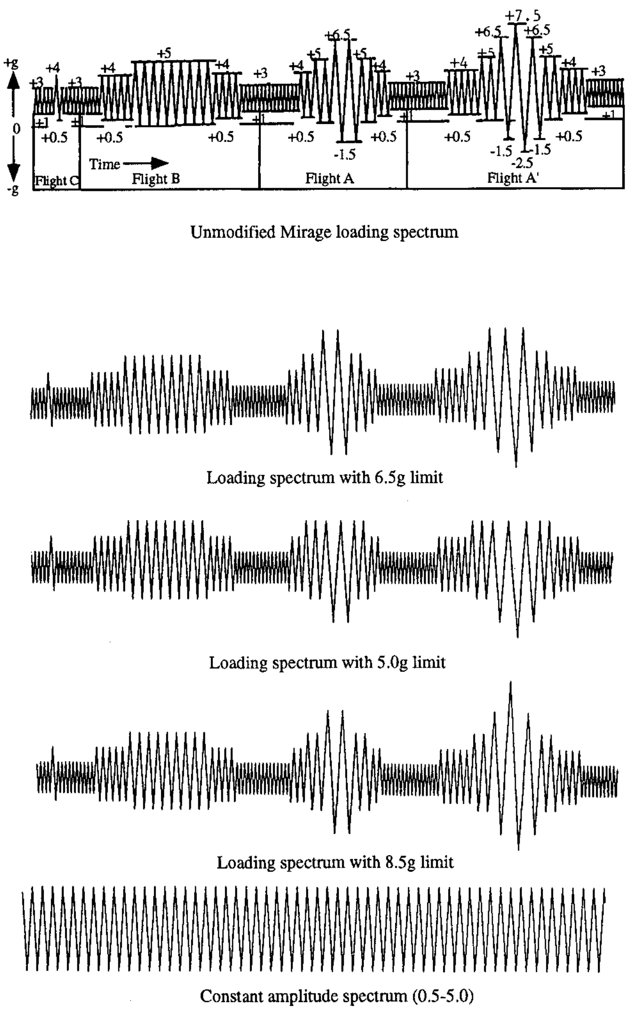

Fig. 3 Various spectrum loadings considered in this study.[15]

trum of 0.5–5.0, unmodified Mirage spectrum (7.5g spectrum), spectrum truncated at +6.5g level (6.5g spectrum), spectrum truncated at +5g level (5g spectrum), and spectrum truncated to +8.5g (8.5g spectrum). The graphical representation of these loading spectrums and details of the loadings for each of the four different flight segment blocks, (A′, A, B, C), which make up the spectrum, are also shown in Fig. 3. The crack-growth loading cycle curves for these loading spectrums were obtained from Ref. 15 and digitized. These five different spectrums have different values of cycles for final failure.

The FCN completed training at approximately 1510 iterations. The convergence criteria used in training the NN was set at a global error, $E \le 0.000001$. The learning coefficient η and the momentum term α were determined empirically and were set at 0.8 and 0.7, respectively. Details of different learning algorithms and implementation procedures can be found in Refs. 9 and 10.

After the network has completed the training phase, a set of test data that the network had not seen before was presented during the testing phase. The set of data used for testing had changes in g of the spectrum as well as changes in flight segment blocks of the spectrum. The testing and learning procedures were implemented on a SUN/SPARC2 system. The results are presented in the next section.

The MPN is also modeled similar to the FCN model using a back-propagation network as described earlier. However, unlike the FCN, this network has only three inputs and three outputs. As shown in Fig. 1, MPN has only one hidden layer with 17 units. The input to the network consists of da/dN,

ΔK, r, and the output from the network is the three material parameters, C, m, and n (see Fig. 1). The network was trained with constant amplitude and spectrum loadings of 7.5 and 6.5g, and tested with 5.0 and 8.5g spectrum loadings. The convergence criteria for the network, learning coeffients, and momentum term values used for MPN are similar to the ones used for the FCN.

V. Results and Discussion

Figure 4 shows the results of crack-growth cycles behavior after training the network for an accuracy of 0.000001 between the experimental data and neural network predictions. The results are in good agreement with the experimental data for all the five different loading spectrums. It can be seen from Fig. 4 that the network has learned the crack-growth behavior for the five types of spectrum loadings that it has trained in.

With limited experimental data on constant amplitude loadings, the NN was not able to generalize fully. No other experimental data was available for training to generalize the NN for constant amplitude as well as spectrum loadings. To enhance the predictive capabilities of NN, analytical results for constant loading were used. The following experiments were done:

A. Experiment 1

The crack-growth vs cycles data for 0.45–4.5 and 0.55–5.5 constant amplitude loadings was generated analytically using Eqs. (3) and (11). The NN was trained using this data and the experimental data for the five spectrum loadings shown

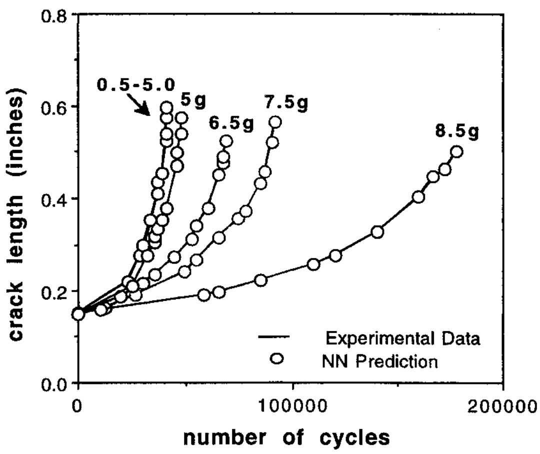

Fig. 4 Comparison of NN predictions with experimental data for the five trained spectrum loadings.

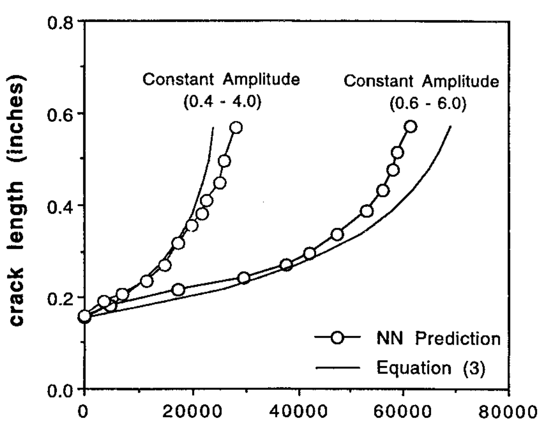

Fig. 5 Comparison of NN predictions with Walker's equation for constant amplitude loadings.

in Fig. 3. This trained NN was then used to predict the crack-growth behavior for 0.4–4.0 and 0.6–6.0 constant amplitude loadings.

Figure 5 shows the NN-predicted crack-growth behavior for 0.4–4.0 and 0.6–6.0 constant amplitude loadings. The crack-growth behavior for these two cases calculated from Eq. (3) is also shown in Fig. 5. There is a 14 and 11% difference between the NN-predicted results and the analytical data for 0.4–4.0 and 0.6–6.0 constant amplitude loadings, respectively. These differences are reasonable as there is a 14% difference between the analytical results and the experimental data obtained in Ref. 15. The results from this experiment illustrate the NN approach for fatigue-crack-growth behavior under constant amplitude loadings with reasonable size of training data.

B. Experiment 2

The objective of this experiment is to compare the NN predictions with the experimental data in Ref. 15. The network was trained with 0.4–4.0 (analytical), 0.55–5.5 (experimental), and 0.6–6.0 (analytical) for constant amplitude loadings, as well as the 5.0, 7.5, and 8.5g spectrum loadings from experiments. The network converged at approximately 50,000 iterations to reach an accuracy of 0.000001. The trained network was then tested for 0.5–5.0 constant amplitude loading as well as for the 6.5g spectrum loading so that a comparison can be made with available experimental data. Figure 6 shows the results of crack-growth vs cycles behavior for these two cases along with the experimental data. A very good agreement is seen for the constant amplitude loading. There is a 10% difference between the NN prediction and the experimental data for the 6.5g spectrum. These results demonstrate the ability of NN to learn and predict the crack-growth vs cycles behavior for constant amplitude as well as for spectrum loadings.

In addition to the above experiments, the following examples were studied to see whether the NN can predict the correct influences for variations in the loading spectrums:

1) Effect of changing g values of the spectrum

7.5g spectrum was reduced to 4.0g spectrum
7.5g spectrum was reduced to 6.0g spectrum
7.5g spectrum was increased to 9.5g spectrum

2) Effect of changing the sequence of blocks in the loading spectrum

Loading flights A and A′ were interchanged (CBA′A)
Loading flights A and B were interchanged (CABA′)
Loading flights B and C were interchanged (BCAA′)

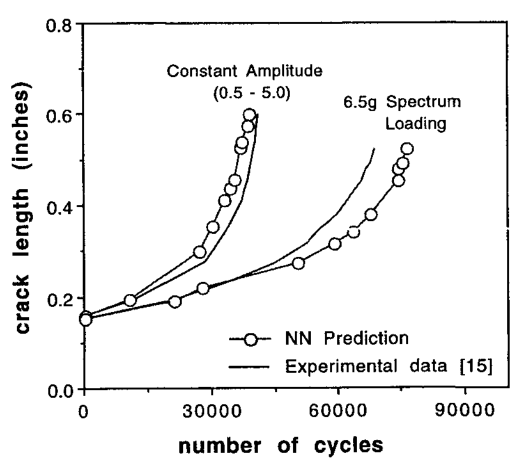

Fig. 6 Comparison of NN predictions with experimental data[15] for constant amplitude (0.5–5.0) and 6.5g spectrum loadings.

Figure 7a shows the NN-predicted crack-growth cycles (a vs n) behavior for 4.0 and 6.0g spectrums. The original experimental data for 5.0 and 6.0g spectrum loadings are also shown in the same figure for relative comparison. It can be seen from Fig. 7a that when the 7.5g spectrum was reduced to 4.0g, the fatigue life was reduced from 91,962 cycles to 44,900 cycles. Similarly, when the loading spectrum was decreased from 7.5 to 6.0g, the fatigue life was decreased from 91,962 cycles to 61,645 cycles. These NN-predicted results are reasonably within the experimental data range. The effect of increasing the 7.5g loading spectrum to 9.5g resulted in a twofold increase (190,000 cycles as compared to 91,962 cycles) in fatigue life (see Fig. 7b). Even though the NN-predicted results for the 9.5g spectrum are higher than those obtained for the 8.5g spectrum, there is a possibility that fracture could take place at the 9.5g peak load, thus significantly reducing the crack-growth life. Since there is no fracture criterion in the NN architecture, the NN approach has no means of determining if fracture would occur earlier at 9.5g. This is the limitation of the proposed NN method.

Table 1 demonstrates the effect of changing the sequence of flight blocks in the 5, 6.5, 7.5, and 8.5g loading spectrums. It can be seen from Table 1 that changing the sequence of flight blocks reduced the fatigue-crack behavior as compared to original experimental data for all the spectrums considered. The flight-block sequence CBA'A has greater effect on fatigue-crack-growth behavior for 6.5, 7.5, and 8.5g spectrums, whereas the flight-block sequence CABA' has greater effect for the 5g spectrum. This is because a higher load was applied in the loading sequences, which will drastically reduce the crack-growth behavior. The flight sequence BCAA' has a lesser effect for all the spectrum loadings. The effect of changing the sequence of flight loadings has a greater impact on higher g than lower g. For the four spectrums considered, the fatigue life was reduced to 64% for 8.5g spectrum when the flight sequence was changed to CBA'A from the original sequence CBAA'. This demonstrates the usefulness of the NN approach for studying the effect of flight sequence loadings on the fatigue-crack-growth behavior.

Table 1 Percentage reduction in NN predicted fatigue life corresponding to a critical crack size of 0.55 in. for different variations in the sequence of blocks in spectrum loadings

	Spectrum, g			
Flight sequence	5	6.5	7.5	8.5
Original spectrum				
CBAA'	100.0	100.0	100.0	100.0
CBA'A	5.7	24.0	42.0	64.0
CABA'	7.5	18.0	32.0	31.0
BCAA'	3.4	8.0	12.0	0.8

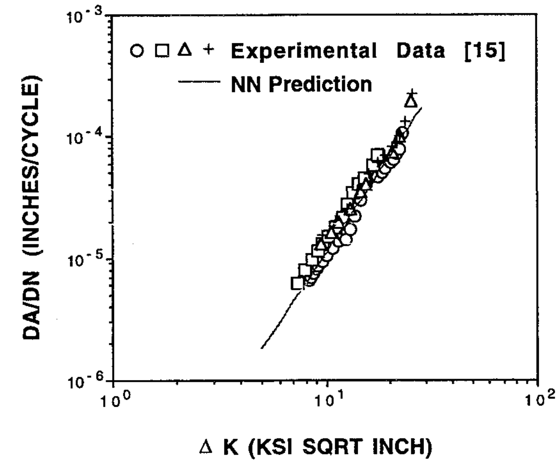

Fig. 8 Comparison of MPN predictions of fatigue-crack-growth rate behavior with experimental data.[15]

The above experiments demonstrate that the fatigue-crack-growth behaviors predicted from NN are reasonable and it provided the correct trends for different variations considered in the spectrum loadings, even with limited training data. The results of NN predictions from these limited studies demonstrate that the network was able to learn the relationship between crack growth and the number of loading cycles for different variations in the loading spectrums as well as sequence of flight loadings. For more accurate predictions, a larger training set is needed.

Fatigue lives are very sensitive to subtle changes in the magnitude and sequence of uncertain overloads that might be large as compared to the remaining cyclic loads in the loading spectrum. It is known that tensile overloads increase fatigue lives, provided that it does not cause immediate fracture. A large training set with a variety of overloads with different magnitude and sequence are required for training the NN before any generalization can be made and applied to estimate the fatigue life of cracked structural components under complex loadings.

Figure 8 shows the fatigue-crack-growth rate vs ΔK curve predicted from MPN using the material parameters along with the experimental data obtained for constant amplitude tests.[15] These material constants are $C = 2.4376 \times 10^{-8}$, $n = 2.6$, and $m = 0.6$. A good agreement is seen even though the input data size is very small. In order to see how the stress ratio will affect the material constants, the results for different values of stress ratio for all the spectrums were obtained. It was found that the stress ratio has no effect on the material constants. This is expected because the material parameters should not change for various spectrums loadings.

a)
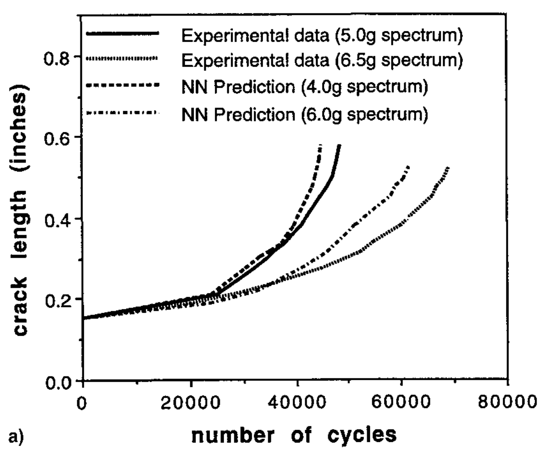

b)
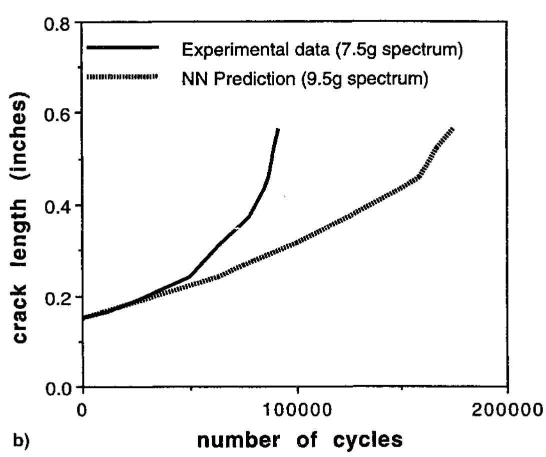

Fig. 7 Comparison of NN predictions for variations in g values in the loading spectrums: a) 4.0 and 6.0g and b) 9.5g spectrums.

VI. Conclusions

A back-propagation neural network is developed to represent the fatigue-crack-growth behavior under aircraft spectrum loadings. Predictions obtained from NN are in good agreement with the experimental data for five different types of spectrum loadings considered. The FCN was tested against variations in g spectrums as well as the sequence of flight loadings. The results of NN-predicted fatigue-crack-growth behavior seem reasonable for generalization, even with limited training data. The material parameters predicted from MPN are in good agreement with the experimental data for constant amplitude tests. Overall, the predictions from this limited study demonstrate the feasibility of the NN approach to study fatigue-crack-growth behavior. However, there are limitations in the present NN approach due to drastic changes in fatigue lives for subtle changes in the magnitude and sequence of uncertain overloads in the loading spectrum as well as not predicting the fracture. Based on the limited performance of the NN method developed in this study, it is possible that this approach can be extended to estimate the fatigue life of arbitrary cracked structural components under complex loadings in real time. More research than presented in this study is needed before such realistic predictions can be made.

Acknowledgments

The authors thank A. F. Grandt Jr., School of Aeronautics and Astronautics, Purdue University, for his helpful suggestions and for making the M.S. Thesis available. The authors thank the reviewers for their valuable comments.

References

[1]Mann, J. Y., Machin, A. S., and Pell, R. A., "Fatigue Crack Propagation in Mirage 1110 Wing Main Spar Specimens and Effects of Spectrum Truncation on Life," Defense Sciences and Technology Organization, Aeronautical Research Labs., Structures Rept. 405, Melbourne, Australia, 1984.

[2]Probst, E. P., and Hillberry, B. M., "Fatigue Crack Delay and Arrest Due to Single Peak Tensile Overloads," *AIAA Journal*, Vol. 12, No. 3, 1974, pp. 330–335.

[3]Trebules, V. W., Jr., Roberts, R., and Hertzberg, R. W., "Effect of Multiple Overloads on Fatigue Crack Propagation in 2024-T3 Aluminum Alloy," *Progress in Flaw Growth and Fracture Testing*, American Society for Testing and Materials, ASTM STP 536, 1973, pp. 115–146.

[4]Elber, W., "The Significance of Crack Closure," *Damage Tolerance in Aircraft Structures*, American Society for Testing and Materials, ASTM STP 486, 1971, pp. 230–242.

[5]Palakal, M., and Zoran, M. J., "A Neural Network Based Learning System for Speech Processing," *Expert Systems with Applications: An International Journal*, Pergamon, New York, 1990, pp. 59–71.

[6]Handelman, D. A., Lane, S. H., and Gelfand, J. J., "Integrating Neural Networks and Knowledge-Based Systems for Intelligent Robotic Control," *IEEE Control Systems Magazine*, April 1990, pp. 77–86.

[7]Hajela, P., and Berke, L., "Neurobiological Computational Models in Structural Analysis and Design," *Proceedings of the AIAA 31st Structures, Structural Dynamics, and Materials Conference* (AL), AIAA, Washington, DC, 1990, pp. 345–355.

[8]Rumelhart, D. E., Hinton, G. E., and McClelland, J. L., "A General Framework for Parallel Distributed Processing," *Parallel Distributed Processing, Vol. 1: Foundations*, Massachusetts Inst. of Technology Press, Cambridge, MA, 1986.

[9]Lippmann, R. P., "An Introduction to Computing with Neural Nets," *IEEE Acoustic, Speech, and Signal Processing Magazine*, Vol. 4, No. 2, 1987, pp. 4–22.

[10]Freeman, J. A., and Skapura, D. M., "Neural Networks: Algorithms, Applications, and Programming Techniques," Addison–Wesley, Reading, MA, 1991.

[11]Ghaboussi, J., Garrett, J. H., Jr., and Wu, X., "Knowledge-Based Modeling of Material Behavior with Neural Network," *Proceedings of the ASCE, Journal of Engineering Mechanics*, Vol. 117, No. 1, 1991, pp. 132–153.

[12]Pidaparti, R. M. V., and Palakal, M. J., "A Material Model for Composites Using Neural Networks," *AIAA Journal*, Vol. 31, No. 8, 1993, pp. 1533–1535.

[13]Merrill, W., and Troudet, T., "Neural Network Would Estimate Fatigue Life," NASA Tech. Briefs, March 1993, pp. 26, 27; also Troudet, T., and Merrill, W., "A Real Time Neural Net Estimator of Fatigue Life," NASA TM 103117, June 1990.

[14]Walker, K., "Effects of Environment and Complex Load History on Fatigue Life," American Society for Testing and Materials, ASTM STP 462, 1970, pp. 1–14.

[15]Walker, K. F., "The Effect on Fatigue Crack Growth Under Spectrum Loading of an Imposed Placard g Limit," M.S. Thesis in Aeronautics and Astronautics, Purdue Univ., West Lafayette, IN, 1987.